3-1-2020

Non-Heisenberg magnetism in a quaternary spin-gapless semiconductor

R. Choudhary
Indian Institute of Technology, Mandi

A. Kashyap
Indian Institute of Technology, Mandi

Durga Paudyal
Ames Laboratory, durga@ameslab.gov

D. J. Sellmyer
University of Nebraska, Lincoln

R. Skomski
University of Nebraska, Lincoln

Non-Heisenberg magnetism in a quaternary spin-gapless semiconductor

Abstract

Understanding of spin-gapless semiconductors with fully spin-polarized charge carriers is critically important because of their promise for spintronic applications. Here, we report non-collinear spin structures, magnetic ground state, and effective exchange interactions of the spin-gapless semiconductor CoFeCrAl investigated with noncollinear density functional calculations. The ground state of CoFeCrAl is ferrimagnetic and has a spin configuration with ↓ Fe, ↑ Co and ↑ Cr spins. In our constrained calculations, the magnetizations of the Fe, Co, and Cr sublattices are rotated by various angles θ, which give rise to three sets of noncollinear spin structures. For all three elements, the magnetic energy increases with the angle, which reconfirms the ferrimagnetic spin structure. During rotation, the magnitudes of the Co and Cr spins remain almost unchanged, whereas that of Fe strongly decreases as a function of the angle θ. This indicates that the finite-temperature behavior of CoFeCrAl is characterized by a pronounced non-Heisenberg behavior of the ↓ Fe moments, whereas the ↑ Co and ↑ Cr moments are Heisenberg-like. We discuss how this feature affects the finite-temperature behavior of the alloy beyond the commonly considered intersublattice Heisenberg exchange.

Keywords

Spin-gapless semiconductor, constrained spins, atomic moment, exchange-interaction constant

Disciplines

Materials Science and Engineering | Quantum Physics

Non-Heisenberg Magnetism in a Quaternary Spin-Gapless Semiconductor

R. Choudhary,[1-3] A. Kashyap,[1] D. Paudyal,[3] D. J. Sellmyer,[2] and R. Skomski[2]

[1]*School of Basic Sciences, Indian Institute of Technology, Mandi, Himachal Pradesh, India*
[2]*Department of Physics and Astronomy and NCMN, University of Nebraska, Lincoln, NE, USA*
[3]*Ames Laboratory, U.S. Department of Energy, Iowa State University, Ames, IA, USA*

Abstract

Understanding of spin-gapless semiconductors with fully spin-polarized charge carriers is critically important because of their promise for spintronic applications. Here, we report non-collinear spin structures, magnetic ground state, and effective exchange interactions of the spin-gapless semiconductor CoFeCrAl investigated with noncollinear density functional calculations. The ground state of CoFeCrAl is ferrimagnetic and has a spin configuration with ↓ Fe, ↑ Co and ↑ Cr spins. In our constrained calculations, the magnetizations of the Fe, Co, and Cr sublattices are rotated by various angles θ, which give rise to three sets of noncollinear spin structures. For all three elements, the magnetic energy increases with the angle, which reconfirms the ferrimagnetic spin structure. During rotation, the magnitudes of the Co and Cr spins remain almost unchanged, whereas that of Fe strongly decreases as a function of the angle θ. This indicates that the finite-temperature behavior of CoFeCrAl is characterized by a pronounced non-Heisenberg behavior of the ↓ Fe moments, whereas the ↑ Co and ↑ Cr moments are Heisenberg-like. We discuss how this feature affects the finite-temperature behavior of the alloy beyond the commonly considered intersublattice Heisenberg exchange.

Keywords: Spin-gapless semiconductor**,** constrained spins, atomic moment, and exchange-interaction constant.

I. INTRODUCTION

A new class of materials called spin gapless semiconductors (SGS) [1–3] exhibits an open band gap for one spin channel and a closed one for the other, resulting in unique half-metallic and semiconducting properties simultaneously. These materials may provide an effective bridge between semiconducting and half-metallic ferromagnets [4]. These materials fall under the class of Heusler compounds, which include magnetically ordered materials exclusively composed of elements with zero magnetization, have fascinated scientists for more than a century [5]. Heusler's original work includes alloys such as Mn-Bi [5], but soon afterward it became clear that the archetypal Heusler compounds were of the cubic Heusler ($L2_1$), semi-Heusler, or inverted-cubic Heusler types. Recently, more complicated Heusler-type structures, such as tetragonal and quaternary Heuslers, have attracted much attention in spin electronics, especially in the context of half-metallic ferromagnetism and spin-gapless semiconductivity. One example is the Y-ordered quaternary compound CoFeCrAl (prototype LiMgPdSn, space group $F\bar{4}3m$), which was predicted by Özdoğan *et al.* [6] to be a spin-gapless semiconductor (SGS). Such materials are of interest in spin electronics, due to high carrier mobility, voltage-tunable spin polarization, and switchability between *n*- and *p*-type conduction mechanisms. Recently, a phase of this type was shown to exist experimentally, albeit with the substantial disorder and possibly having the $L2_1$ rather than Y structure[7,8].

The spin structure of the quaternary SGS is only partially understood. The alloys contain several magnetic sublattices, a situation also encountered in many other Heusler alloys. They can be considered as ferrimagnets in lowest order [6,9,10], although noncollinear spin structures are not uncommon in Heuslers [11–13]. Experiment (Fig. 3 in Ref. 3) reveals inflections in the temperature dependence of the magnetization that typical for many-sublattice magnets. The corresponding mechanism is well-understood for localized Heisenberg moments [14,15], exemplified by the well-known $M(T)$ behavior of garnets [16]. However, it is by no means clear that the involved atomic spins are of the Heisenberg type. First, Heusler alloys are essentially itinerant magnets, that is, the low-temperature 3*d* moments are delocalized throughout the crystal, as contrasted for example to the localized character of rare-earth 4*f* moments. At finite temperatures, the itinerant 3*d* moments acquire some localized character due to thermal randomization and become more Heisenberg-like[17]. Even at zero temperature, the magnetic-

moment density is quasi-localized for some atoms, that is, narrowly centered around the nucleus [9].

A second point and the main focus of this paper is that the Heisenberg model requires atomic moments to remain *constant* during spin rotation. In the classical limit, this is easily achieved by normalizing the vector $S^2 = 1$, whereas the corresponding quantum-mechanical expression is $\hat{S}^2 = S(S + 1)$. This condition is reasonably well satisfied in a number of itinerant magnets, such as Co, but not met at all in very weak itinerant ferromagnets (VWIF), such as $ZrZn_2$ [18–20]. Any attempt to rotate an atomic spin in a VWIF leads to the collapse of the magnetic moment, that is, to $S^2 \approx 0$, at some misalignment angle. Furthermore, S and $\hat{S}^2 = S(S + 1)$ are not very well-defined in itinerant magnets, due to quantum fluctuations associated with the hopping of correlated 3*d* electrons between atoms [21]. Density functional theory is a much better starting point for itinerant magnets, where electron correlations are weak.

In this paper, we show that the magnetism of CoFeCrAl is intermediate between Heisenberg ferromagnetism and very weak itinerant ferromagnetism. We use constrained density functional theory to fix the atomic moments in various directions, calculate the atomic moments as a function of the magnetization angle between neighboring atoms, and determine the effective interatomic exchange $\mathcal{J}_{ij}$. The exchange is obtained by fitting the DFT predictions to the angular dependence of the classical Heisenberg model, $\mathcal{J}_{ij} \cos(\theta_i - \theta_j)$. One consequence of this unique mechanism is the reduction of the ordering temperature compared to the Heisenberg prediction.

II. COMPUTATIONAL METHOD

The collinear calculations are performed using density functional theory (DFT) [22] and the noncollinear spin orientations of CoFeCrAl are investigated using constrained DFT calculations[23,24]. All the calculations are based on the projector augmented wave (PAW)[25] implemented in the Vienna *ab-initio* simulation package (VASP) [26,27], and a generalized gradient approximation (GGA) has been used for the exchange and correlation functional [28]. To check the accuracy of our method, we performed density of states (DOS) and magnetic-moment calculations for CoFeCrAl, discussed in our earlier work [10], which agree with previous experimental and theoretical results [29,30]. Experimental lattice parameters for CoFeCrAl i.e. $a = b = c = 5.75$ Å [5] were used to relax the structures. Relaxed parameters are $a = b = c = 5.69$

Å. The convergence scale for the self-consistent calculations is fixed to 10^{-7} eV for the total energy per unit cell. The Brillion zone integration uses a 17 × 17 × 17 Monkhorst *k*-point grid [31] for self-consistent calculations and a 13 × 13 × 13 Monkhorst *k*-point grid for the constrained non-collinear calculations. For the electron wave functions, we have used an energy cutoff of 350 eV. These grids and energy cutoff are sufficiently large to ensure high accuracy. The considered Y-ordered CoFeCrAl structure has Co, Fe, Cr and Al on the Wyckoff positions 4a (0, 0, 0), 4b (½, ½, ½), 4c (¼, ¼, ¼) and 4d (¾, ¾, ¾) respectively.

III. RESULTS AND DISCUSSION

We first performed collinear calculations to check the basic spin structure, already discussed in our previous report [10]. The magnetic properties of SGS CoFeCrAl and DOS confirm that the compound has ferrimagnetic spin-gapless semiconductor behavior. SGS CoFeCrAl has a magnetic moment of 2.018 μ_B per f.u. and minority band gap is 0.33 eV. The total moment is in good agreement with the experimental value [7,29] of ~2 μ_B per f.u. Fig. 1 shows the configuration with the lowest energy, namely a ferrimagnetic structure with moments where the spin directions are Cr↑, Co↑, and Fe↓ and the DOS of CoFeCrAl. The unit cell contains 4 formula units (16 atoms). Four different starting configurations have been used in the calculation, covering all possible ferro- and antiferromagnetic intersublattice alignments and all configurations converge to the ferrimagnetic structure of Fig. 1(a). The moments per Cr, Co, and Fe atom are 1.66 μ_B, 0.94 μ_B, and -0.56 μ_B, respectively in the good agreement with previous predicted moment values [29] i.e. m_{Cr} = 1.78 μ_B, m_{Co} = 0.94 μ_B and m_{Fe} = -0.63 μ_B.

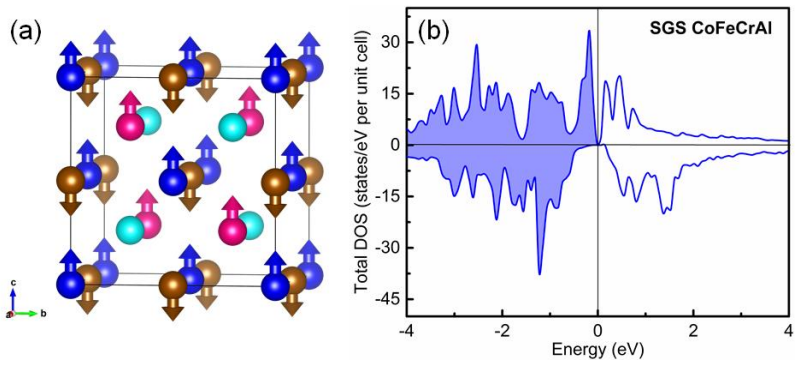

Fig.1. **(a)** A unit cell of CoFeCrAl, the arrows indicating the stable ferrimagnetic spin configuration. The atoms are Fe (brown), Co (blue), Cr (pink), and Al (cyan). **(b)** Total densities of states for CoFeCrAl.

A. Constrained non-collinear calculations

Non-collinear calculations were performed by constraining the atomic spins at an angle θ. Schematic Fig. 2 shows the constrained spin structures considered in this paper. Three different spin configurations were considered. Spin structures I, II and III have Fe (a), Co (b) and Cr (c) spin rotated with respect to the stable spin structure at angles of θ = 15º, 30º, 45º, 60º. The total energy per unit cell and atomic moments were obtained as a function of θ. In all cases, the energy increases with rotation angle while the moment decreases. Fig. 3 shows the energy change due to rotation; the energy zero corresponds to the ferrimagnetic ground-state spin configuration of Fig. 1. The energy differences of Fig. 3 confirm the ground-state spin configuration is ferrimagnetic.

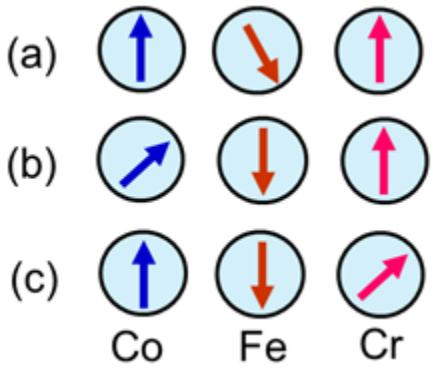

Fig. 2. Schematic constrained non-collinear spin configurations in CoFeCrAl: (a) all Fe spins are rotated at an angle θ (b) all Co spins are rotated at an angle θ (c) all Cr spins are rotated at an angle θ. The angles considered in the calculations are θ = 15º, 30º, 45º, 60º.

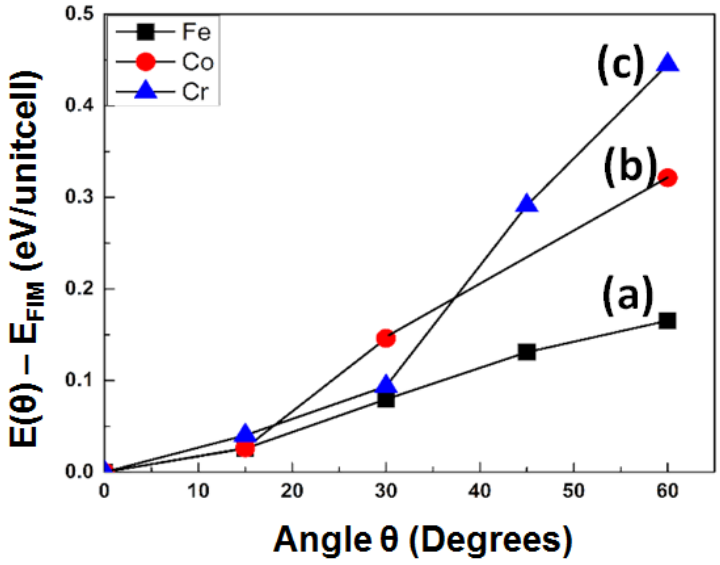

Fig. 3. Energy per unit cell as a function of the Fe, Co, and Cr rotation angles. The energy zero corresponds to the ferrimagnetic ground state of Fig. 1.

Since $\cos(\theta_i - \theta_j)$ and $\theta_j = 0$ in the present calculations, the Heisenberg model corresponds to a cosine-like dependence $E(\theta)$. Fig. 3 shows that this dependence is approximately realized for Cr and Co, but that of Fe is almost linear. The non-Heisenberg behavior of the Fe sublattice indicates that the Heisenberg condition $S^2 = const.$ is violated for the Fe atoms.

Fig. 4 shows the angular dependence of the atomic moments of Fe, Co, and Cr in the constrained spin structures. All moments decrease with the angle, but for Co and Cr, the decrease from 0º to 60º is only about 10%, whereas the decrease for Fe is approximately 70%. This indicates a pronounced non-Heisenberg behavior of the Fe moments, in contrast to the almost Heisenberg-like Co and Cr moments. The strongly reduced Fe moment lowers the energy compared to the ferrimagnetic ground state and is responsible for the flat and nearly linear $E(\theta)$ dependence for Fe.

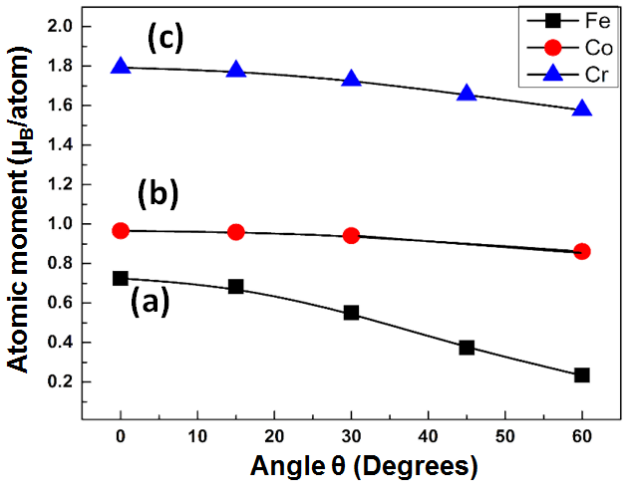

Fig. 4. Angular dependence of the atomic moments of Fe, Co, and Cr. The curves correspond to the noncollinear structures of Fig. 2 (a-c).

B. Exchange interactions

So far, non-collinear calculations for the finite-temperature behavior of CoFeCrAl has not been studied. The energies and moments of Figs. 3 and 4, respectively, strongly affect the Curie temperature, generally reducing T_c. An extreme case is very weak-itinerant ferromagnetic, where the energy associated with moment formation is more important than the energy associated with spin rotations [18–21,32]. The effect can be described approximately by introducing effective intersublattice exchange constants $\mathcal{J}^*_{ij}$ that corresponds to the Hamiltonian

$$\mathcal{J}_{eff} = -\Sigma_{ij}\, \mathcal{J}^*_{ij}\, \boldsymbol{\mu}_i \cdot \boldsymbol{\mu}_j \qquad (1)$$

Here $\boldsymbol{\mu}_i$ is the unit vector along the direction of magnetic moment at site i. Since the magnitude of $\boldsymbol{\mu}_i$ is fixed, non-Heisenberg effects are mapped onto a reduction of $\mathcal{J}^*_{ij}$, which results in a reduced Curie temperature T_c.

The energies obtained in our DFT calculations correspond to summations of the type $\mathcal{J}_{eff}(i) = \Sigma_j\, \mathcal{J}^*_{ij}$. Table I lists $\mathcal{J}_{eff}$ for Fe, Cr, and Co as a function of angle. The calculation for the rotating angle of 45^0 for Co-spin was highly unstable. This gives rise to a false local-minima. The self-consistent solution of multisublattice interaction problem, that is, finding $M(T)$ and T_c from the $\mathcal{J}^*_{ij}$, is highly nontrivial, even on a mean-field level. In addition to the mean-field equations being

nonlinear [5], the $\mathcal{J}^*_{ij}$ exhibit a temperature dependence through the angles θ of the thermally fluctuating spins.

Table I. Effective exchange-interaction constants, $\mathcal{J}_{eff}$ for Fe, Co and Cr in the constrained noncollinear structures of Fig.2 (a-c).

Angle (θ)	$\mathcal{J}_{eff}$ (meV)		
	Fe	Co	Cr
15º	94.5	96.5	147.8
30º	74.2	136.2	87.4
45º	55.0	-	124.2
60º	41.3	80.4	111.2

Experimentally, the intersublattice interactions manifest themselves as bumps, inflections, and zeros in the $M(T)$ curves [14,15]. Such deviations from simple ferromagnetism are visible in the experimental $M(T)$ curves [7], and both Heisenberg and non-Heisenberg interactions contribute to these features. However, quantitative comparison with experiment is difficult, because the $M(T)$ curves depend on the chemical disorder which is affected by heat treatment, whereas Eq. (1) assumes a perfect lattice.

IV. CONCLUSIONS

In summary, we have analyzed how non-Heisenberg interactions affect the spin structure of the quaternary Heusler compound CoFeCrAl, a spin-gapless semiconductor having a ferri-magnetic ground state. Constrained noncollinear DFT calculations have been used to calculate the magnetic energies and atomic moments as a function of the misalignment angle. The Co and Cr spins are Heisenberg-like, whereas the Fe moment strongly decreases with increasing angle. Our analysis goes beyond the conventional analysis of ferrimagnets in terms of Heisenberg-type intersublattice interactions and corresponds to a Curie-temperature reduction due to the fluctuating Fe moments.

ACKNOWLEDGMENTS

This research has been supported by DOE-BES (DE-FG02-04ER46152, R. S., and D. J. S), the Nebraska Center for Materials and Nanoscience, and the Holland Computing Center and by Nano Mission, DST, India (SR/NM/NS-1198/2013, R. C., and A. K.). This research is supported in part

by the Critical Materials Institute, an Energy Innovation Hub funded by the U.S. Department of Energy, Office of Energy Efficiency and Renewable Energy, Advanced Manufacturing Office.

References

[1] X.L. Wang, Proposal for a New Class of Materials: Spin Gapless Semiconductors, Phys. Rev. Lett. 100 (2008) 156404.

[2] X. Wang, Z. Cheng, J. Wang, X.L. Wang, G. Liu, Recent advances in the Heusler based spin-gapless semiconductors, J. Mater. Chem. C. 4 (2016) 7176–7192.

[3] Q. Gao, I. Opahle, H. Zhang, High-throughput screening for spin-gapless semiconductors in quaternary Heusler compounds, Phys. Rev. Mater. 3 (2019).

[4] H. van Leuken, R.A. de Groot, Half-Metallic Antiferromagnets, Phys. Rev. Lett. 74 (1995) 1171–1173.

[5] F. Heusler, Über Manganbronze und über die Synthese magnetisierbarer Legierungen aus unmagnetischen Metallen, Zeitschrift Für Angew. Chemie. 17 (1904) 260–264.

[6] K. Özdoğan, E. Şaşıoğlu, I. Galanakis, Slater-Pauling behavior in LiMgPdSn-type multifunctional quaternary Heusler materials: Half-metallicity, spin-gapless and magnetic semiconductors, J. Appl. Phys. 113 (2013) 193903.

[7] P. Kharel, W. Zhang, R. Skomski, S. Valloppilly, Y. Huh, R. Fuglsby, S. Gilbert, D.J. Sellmyer, Magnetism, electron transport and effect of disorder in CoFeCrAl, J. Phys. D. Appl. Phys. 48 (2015) 245002.

[8] Y. Jin, P. Kharel, S.R. Valloppilly, X.-Z. Li, D.R. Kim, G.J. Zhao, T.Y. Chen, R. Choudhary, A. Kashyap, R. Skomski, D.J. Sellmyer, Half-metallicity in highly L21-ordered CoFeCrAl thin films, Appl. Phys. Lett. 109 (2016).

[9] L. Wollmann, S. Chadov, J. Kübler, C. Felser, Magnetism in cubic manganese-rich Heusler compounds, Phys. Rev. B. 90 (2014) 214420.

[10] R. Choudhary, P. Kharel, S.R. Valloppilly, Y. Jin, A. O'connell, Y. Huh, S. Gilbert, A. Kashyap, D.J. Sellmyer, R. Skomski, Structural disorder and magnetism in the spin-gapless semiconductor CoFeCrAl, AIP Adv. 6 (2016) 56304.

[11] O. Meshcheriakova, S. Chadov, A.K. Nayak, U.K. Rößler, J. Kübler, G. André, A.A. Tsirlin, J. Kiss, S. Hausdorf, A. Kalache, W. Schnelle, M. Nicklas, C. Felser, Large Noncollinearity and Spin Reorientation in the Novel Mn_2RhSn Heusler Magnet, Phys. Rev. Lett. 113 (2014) 087203.

[12] S. Paul, S. Ghosh, B. Sanyal, Emergence of spin spiral magnetic order in Mn based inverse Heusler alloys, J. Phys. Condens. Matter. 26 (2014) 196004.

[13] J. Enkovaara, A. Ayuela, J. Jalkanen, L. Nordströ, R.M. Nieminen, First-principles calculations of spin spirals in Ni_2MnGa and Ni_2MnAl, Phys. Rev. B. 67 (2003) 054417.

[14] J. S. Smart, Effective Field Theories of Magnetism, Saunders, Philadelphia, 1966.

[15] R. Skomski, Simple Models of Magnetism, University Press, Oxford, 2008.

[16] S. Chikazumi, Physics of Magnetism., Wiley, New York, 1964.

[17] P. Fulde, Electron correlations in molecules and solids, Springer-Verlag, 1991.

[18] E.P. Wohlfarth, Very weak itinerant ferromagnets; Application to $ZrZn_2$, J. Appl. Phys. 39 (1968) 1061–1066.

[19] P. Mohn, E.P. Wohlfarth, The Curie temperature of the ferromagnetic transition metals and their compounds, J. Phys. F Met. Phys. 17 (1987) 2421–2430.

[20] P. Mohn, Magnetism in the Solid State, Springer, Berlin, 2003.

[21] R. Skomski, P. Kumar, B. Balamurugan, B. Das, P. Manchanda, P. Raghani, A. Kashyap, D.J. Sellmyer, Exchange and magnetic order in bulk and nanostructured Fe_5Si_3, J. Magn. Magn. Mater. 460 (2018) 438–447.

[22] W. Kohn, L.J. Sham, Self-Consistent Equations Including Exchange and Correlation Effects, Phys. Rev. 140 (1965) A1133–A1138.

[23] P.-W. Ma, S.L. Dudarev, Constrained density functional for noncollinear magnetism, Phys. Rev. B. 91 (2015) 54420.

[24] B. Kaduk, T. Kowalczyk, T. Van Voorhis, Constrained Density Functional Theory, Chem. Rev. 112 (2012) 321–370.

[25] G. Kresse, D. Joubert, From ultrasoft pseudopotentials to the projector augmented-wave

method, Phys. Rev. B. 59 (1999) 1758–1775.

[26] G. Kresse, J. Furthmüller, Efficient iterative schemes for ab initio total-energy calculations using a plane-wave basis set, Phys. Rev. B. 54 (1996) 11169–11186.

[27] J. Hafner, Ab-initio simulations of materials using VASP: Density-functional theory and beyond, J. Comput. Chem. 29 (2008) 2044–2078.

[28] Perdew, Burke, Wang, Generalized gradient approximation for the exchange-correlation hole of a many-electron system., Phys. Rev. B. Condens. Matter. 54 (1996) 16533–16539.

[29] L. Bainsla, A.I. Mallick, A.A. Coelho, A.K. Nigam, B.S.D.C.S. Varaprasad, Y.K. Takahashi, A. Alam, K.G. Suresh, K. Hono, High spin polarization and spin splitting in equiatomic quaternary CoFeCrAl Heusler alloy, J. Magn. Magn. Mater. 394 (2015) 82–86.

[30] J. Nehra, V.D. Sudheesh, N. Lakshmi, K. Venugopalan, Structural, electronic and magnetic properties of quaternary half-metallic Heusler alloy CoFeCrAl, Phys. Status Solidi - Rapid Res. Lett. 7 (2013) 289–292.

[31] H.J. Monkhorst, J.D. Pack, Special points for Brillonin-zone integrations, Phys. Rev. B. 13 (1976) 5188–5192.

[32] T. Moriya, Spin fluctuations in itinerant electron magnetism, Springer-Verlag, 1985.